AIAA SciTech
4-8 January 2016, San Diego, California, USA
54th AIAA Aerospace Sciences Meeting

Quiet Nozzle Concepts for Three-Stream Jets

D. Papamoschou[1], V. Phong[2], J. Xiong[3], and F. Liu[4]
University of California, Irvine, Irvine, CA, 92697

We present a study of three-stream nozzle concepts with potential to reduce takeoff noise of future commercial supersonic aircraft. The concepts were evaluated at realistic cycle conditions in a subscale acoustic facility. Computations solving the Reynolds-Averaged Navier-Stokes equations provided insight into the changes in the flow field that can impact noise generation. The investigation encompassed long- and short-cowl nozzles in coaxial and asymmetric arrangements where the third stream was concentrated in the downward azimuthal direction. In coaxial configurations, addition of the third stream makes a modest impact on the noise emission, with a small benefit at high frequencies in the aft arc. This benefit is more evident in short-cowl nozzles. Asymmetric arrangements involved offsetting the tertiary duct and/or application of an internal wedge-shaped deflector. The asymmetry produces significant noise reduction in the direction of the thickened tertiary flow, and is more effective at cycle conditions with high specific thrust. Reduction of the skewness of the far-field pressure fluctuations suggests suppression of Mach wave radiation by the asymmetric tertiary flow.

I. Introduction

There is renewed interest in the development of supersonic commercial aircraft that will feature low boom and reduced takeoff noise at levels equivalent to those of the subsonic fleet. This activity is illustrated by extensive systems and component studies aimed to achieve aerodynamic efficiency and environmental acceptability[1]. An important factor in this effort is the advent of the variable-cycle engine, which allows control of the bypass ratio and features two- and three-stream architectures[2]. The three-stream implementation is the focus of the present study.

Noise reduction concepts for high-speed jets have taken many forms and have generated a large body of literature. A comprehensive review can be found in a paper by Morris and McLaughlin[3]. Here we focus on fundamental concepts and associated noise reduction methods pertaining to multi-stream jets. The supersonic turbofan engine is bound to operate at a lower bypass ratio than its subsonic versions. This means high exhaust velocities and the associated Mach wave radiation - the sound generated by the supersonic convection of the large-scale turbulent eddies in the jet plume. Suppression of Mach wave radiation is thus essential for achieving the desired reductions in community noise.

Research on supersonic coaxial jets started in the 1970s, with initial emphasis on reduction of shock-cell noise[4]. Significant theoretical, computational, and experimental work followed[6-10], with the models by Tanna and Morris[6] and Fisher *et al.*[7] offering perhaps the most insightful look into the differences between the coaxial jet and the single-stream jet. In particular, these models recognized that sound generation from the inner shear layer is suppressed as long as the inner shear layer is surrounded by an outer potential core. The noise suppression is related to the decrease in the turbulence level due to the reduced shear; and to the lower relative (convective) Mach number of the most energetic eddies, which results in lower radiation efficiency[11]. For practical low-bypass configurations, however, the secondary

[1] Professor, Department Mechanical and Aerospace Engineering, dpapamos@uci.edu, AIAA Fellow.
[2] Research Specialist, Department Mechanical and Aerospace Engineering, vphong@uci.edu, AIAA Member.
[3] Post-Doctoral Researcher, Department Mechanical and Aerospace Engineering, jxiong@uci.edu, AIAA Member
[4] Professor, Department Mechanical and Aerospace Engineering, fliu@uci.edu, AIAA Fellow.

core ends far upstream of the primary core, so most of the primary shear layer is not enveloped by the secondary potential core. Therefore, noise reduction in coaxial jets (compared to the primary stream alone) is marginal unless the secondary to primary nozzle exit diameter ratio is large[12].

The beneficial effect of the secondary flow - namely the reduced sound generation from the primary shear layer - can be extended further downstream by inducing an asymmetry in the nozzle and/or the jet plume that concentrates the secondary flow in the azimuthal direction where noise reduction is desired. Asymmetry in the nozzle entails offsetting the primary and secondary ducts, while asymmetry in the jet plume (issuing from a coaxial arrangement) can be induced by placing deflectors in the secondary stream. These "offset stream" approaches have been investigated for supersonic[13-17] and subsonic[16-19] jets. The acoustic benefit at supersonic speed can be substantial, while it is more moderate at subsonic speed. There is strong evidence that the suppression of sound in these asymmetric jets is largely caused by the reduction in the convective Mach number of the most energetic eddies and the attendant reduction in radiation efficiency[20,21].

Investigations of three-stream jets have been fairly limited to date. A parametric study of small-scale jets, operating at very low bypass ratios associated with tactical engines, encompassed coaxial and non-coaxial configurations[22]. In coaxial nozzles, the tertiary stream had negligible impact on the acoustics. Supplied in an asymmetric fashion, the tertiary stream could suppress noise significantly in the direction of the thickened flow. The best results were obtained by combined asymmetry of the secondary and tertiary nozzles. Large-scale coaxial three-stream acoustic experiments by Henderson[23] were conducted at subsonic exhaust conditions and at bypass ratios around 5. Introduction of the third stream at a velocity lower than that of the secondary stream reduced moderately high-frequency noise. On an equal-thrust basis, there was no acoustic benefit of the three-stream jet over the two-stream jet. A subsequent study by Henderson *et al.*[24] considered a larger variety of nozzle geometries, area ratios and pressure ratios. In axisymmetric arrangements the tertiary stream produced very small impacts on the acoustics; however, when the tertiary nozzle was offset significant reductions were measured in the direction of the thickened flow. The asymmetric distribution of the turbulent kinetic energy was measured using particle image velocimetry and predicted using Reynolds-Averaged Navier-Stokes (RANS) computations.

The present paper reports results from a broad effort to study parametrically the acoustics of three-stream jets compatible with engines of supersonic transports, and to develop predictive methodologies. The focus is on experimental acoustic data of selected nozzle configurations that illustrate some important trends. Where feasible the experimental results are accompanied by RANS predictions of the plume to make qualitative connections between the changes in acoustics and changes in the flow field. Eventually the computational effort is expected to enable quantitative predictions of the noise changes from a given baseline.

II. Experimental Approach

A. Generic Nozzle Design

The objective of the nozzle design process is to generate test articles that enable rapid and accurate testing of a variety of nozzles having characteristics compatible with the exhaust of three-stream, variable-cycle engines envisioned for future supersonic aircraft. The nozzles need to fit the capacity of the UCI Jet Aeroacoustics Facility, a dual-stream jet facility that delivers helium-air mixtures to the primary (core) and secondary (fan) flows of the nozzle. Helium-air mixtures simulate accurately the acoustics and fluid mechanics of hot jets[25]. To accommodate a third stream, the supply of the third stream is the same as that of the second stream with a pressure drop to independently control the total pressure of the third stream.

The sub-millimeter tolerance requirements for the nozzle exit motivated a design where all the nozzle components are built in one piece, using high-definition stereolithography which allows nozzle lips as thin as 0.2 mm. The material used was Accura 60 plastic (3D Systems) with tensile strength in the range of 58-68 MPa. The design comprises a fixed base on which replaceable nozzle attachments are mounted. Figures 1-3 depict various views and design features of a representative nozzle. Measurement of the total pressure of each stream involves thin channels, of 0.75-mm diameter, introduced into support struts in each of the ducts. The channels begin at the outer surface of the attachment, follow an L-shaped path through the struts, and terminate into upstream-facing ports in their respective ducts (Fig. 1).

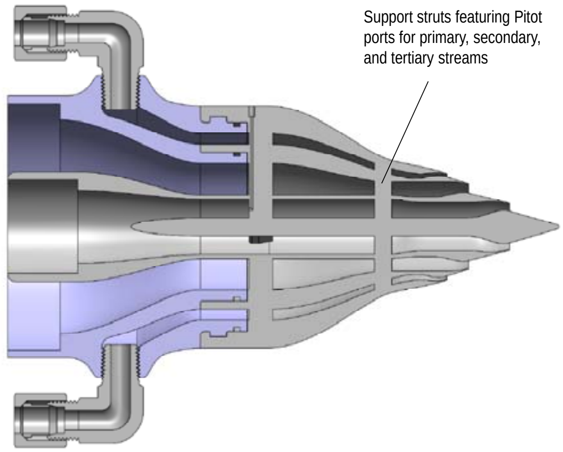

Fig.1 Cross-sectional view of three-stream nozzle.

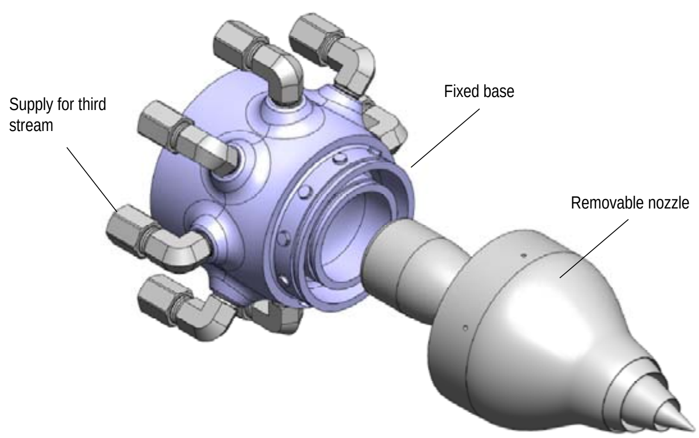

Fig.2 Exploded view of nozzle.

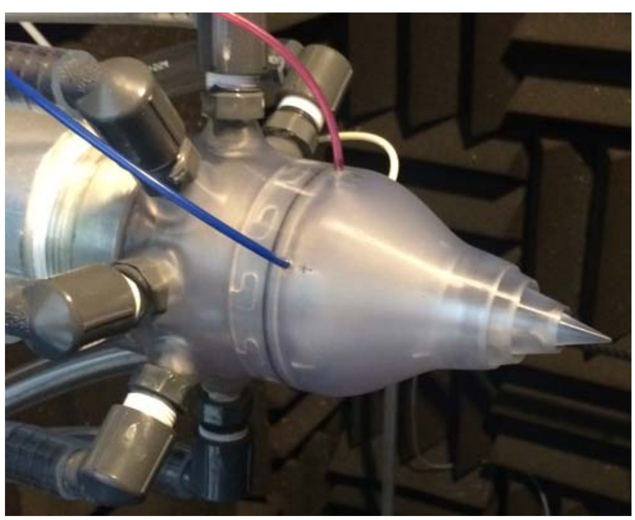

Fig.3 Picture of installed nozzle.

B. Cycle Points
Representative cycle points for three-stream engines were provided to us by NASA Glenn personnel. Table 1 lists five cycles covered in this paper. The cycle name reflects the nozzle pressure ratios (NPRs) and nozzle temperature ratios (NTRs). Cycles 58230 and 88530 are associated with large secondary area ratio and have total bypass ratios near 6.0. Cycle AA530 represents a higher specific thrust, with smaller secondary area ratio and total bypass ratio of 3.6. The outer diameter D_3 of the tertiary nozzle ranged from 31.1 mm to 32.1 mm. The typical Reynolds number of the primary jet was near 750,000. The velocity and Mach number of each cycle point was matched exactly using helium-air mixture jets.

Table 1. Cycle Conditions.

	Primary			Secondary					Tertiary				
Cycle	NPR	NTR	U_1 (m/s)	BPR_2	NPR_2	NTR_2	U_2/U_1	A_2/A_1	BPR_3	NPR_3	NTR_3	U_3/U_1	A_3/A_1
58030	1.50	3.00	429	4.82	1.80	1.25	0.77	2.47	0.00	1.00	1.25	0.00	1.00
58230	1.50	3.00	429	4.82	1.80	1.25	0.77	2.47	1.00	1.20	1.25	0.44	1.00
88030	1.80	3.00	510	3.86	1.80	1.25	0.64	2.47	0.00	1.00	1.25	0.00	1.00
88530	1.80	3.00	510	3.86	1.80	1.25	0.64	2.47	1.26	1.50	1.25	0.54	1.00
AA530	2.02	3.38	590	2.33	2.02	1.34	0.63	1.44	1.31	1.53	1.24	0.48	1.06

C. Specific Nozzles
A large number of coaxial and asymmetric nozzles were designed, evaluated using RANS, and built in the research program. This paper covers a small number of representative configurations. Table 2 provides a summary of the nozzles and their respective cycle points.

Nozzle AXI01U is a scaled-down version of the NASA long-cowl nozzle featured in Ref. 25. Because of the length of the cowl, the tertiary stream is injected far upstream of the primary exit and the tertiary annulus is quite thin. Denoting X_{13} as the distance between the tertiary and primary exit planes, t_3 the tertiary annulus thickness, and $D_{1,\mathrm{eff}}$ the effective (area-based) exit diameter of the primary duct, nozzle AXI01U has $X_{13}/ D_{1,\mathrm{eff}}$ =1.84 and $t_3/D_{1,\mathrm{eff}}$ = 0.079. Under these conditions it is expected that the tertiary stream is fully mixed before it reaches the primary exit, so it is unlikely to induce any significant changes to the fluid mechanics and acoustics of the jet. Indeed, acoustic results to be presented later show that this is the case.

The configuration of AXI01U was deemed ineffective for inducing changes in the acoustics, even with the tertiary stream injected asymmetrically. This motivated the design of a short-cowl version, called AXI02U, in which the secondary and tertiary exits were moved forward. The design change from AXI01U to AXI02U illustrated in Fig. 4. The aforementioned ratios improve to $X_{13}/D_{1,\mathrm{eff}}$ =0.474 and $t_3/D_{1,\mathrm{eff}}$ = 0.099. Although the presence of the tertiary stream in AXI02U was not expected to yield any significant noise reduction, this configuration was the point of departure for creating asymmetric designs.

Asymmetric designs were partly based on UCI's past experience with eccentric nozzle concepts, coupled with guidance from NASA researchers. Early experience in dual-stream jets with asymmetric secondary nozzles[26] showed the promise of fully eccentric ducts or ducts featuring a wedge-shaped deflector. On the other hand, ducts with partial annulus and parallel flow lines produced jets with minimal noise reduction over the corresponding coaxial jet. These observations, and our more recent experience with three-stream low-bypass nozzles[22], influenced the design approach.

Asymmetric shaping of the tertiary duct entailed a partial offset (eccentricity) of the tertiary nozzle and a wedge-shaped internal diverter in the tertiary stream; these concepts were be applied individually and in combination. The point of departure was the short-cowl nozzle, and for each class of nozzles (Table 2) the area ratios were maintained. Each proposed design was carefully evaluated by a RANS computation of the internal and external flows. The internal-flow computation provided an assessment of thrust loss and identified any undesirable flow features, such as flow separation, that would necessitate a redesign. Designs with thrust loss exceeding ~0.25% were eliminated from consideration.

Figure 5 presents nozzle designs for cycle points 58230 and 88530. Each subfigure displays view of the nozzles, characteristic dimensions, and the variation of the tertiary annulus thickness versus azimuthal angle. For designs including wedge deflectors, L denotes the wedge side length and δ the half-angle. Nozzles AXI01U and AXI02U are the long- and short-cowl coaxial designs discussed above. Nozzle ECC01U is based on AXI02U and features an internal wedge deflector for the tertiary stream, with $L/D_{1,\mathrm{eff}}$ =1.695 and δ=25°. Nozzle ECC04U combines the same deflector with an offset of the tertiary duct.

Figure 6 presents nozzle designs for cycle point AA530, which features a lower area ratio for the secondary nozzle. Nozzle AXI03U is a short-cowl coaxial design, similar to AXI02U but with reduced secondary area. Nozzle ECC06U features a shaped offset where thickening of the tertiary annulus is constant over the azimuthal range -90° < ϕ < 90°. The tertiary outer wall is recessed at the top of the nozzle (azimuth angle ϕ = 180°) to prevent formation of a very long thin duct. Nozzle ECC08U adds a wedge deflector to ECC06U, with $L/D_{1,\mathrm{eff}}$ =1.50 and δ=25°.

Table 2. Nozzles.

Cycles and Area Ratios	Axisymmetric Nozzles	Asymmetric Nozzles
58230 and 88530 A_2/A_1=2.47 A_3/A_1=1.00	AXI01U (long cowl) AXI02U (short cowl)	ECC01U ECC04U
AA530 A_2/A_1=1.44 A_3/A_1=1.06	AXI03U (short cowl)	ECC06U ECC08U

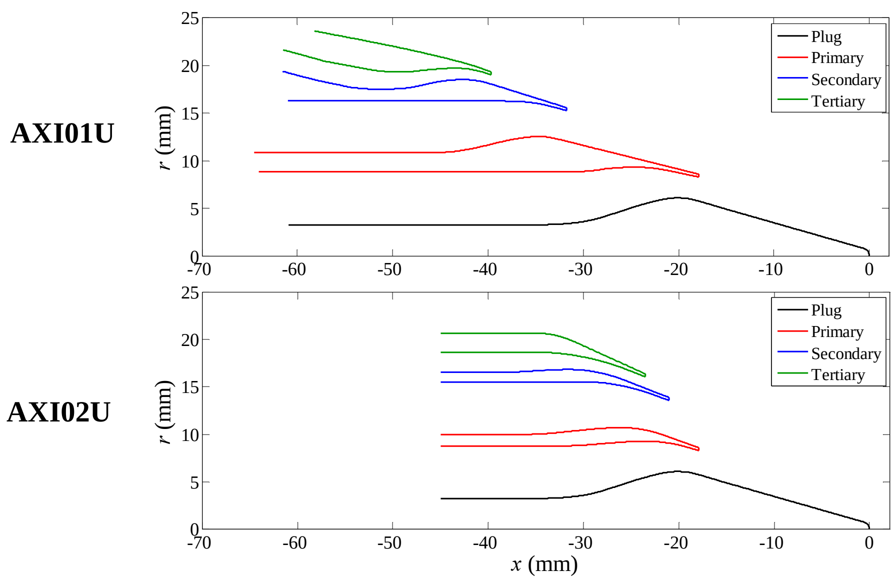

Fig.4 Radial coordinates of long- and short-cowl coaxial nozzles associated with cycle points 58230 and 88530.

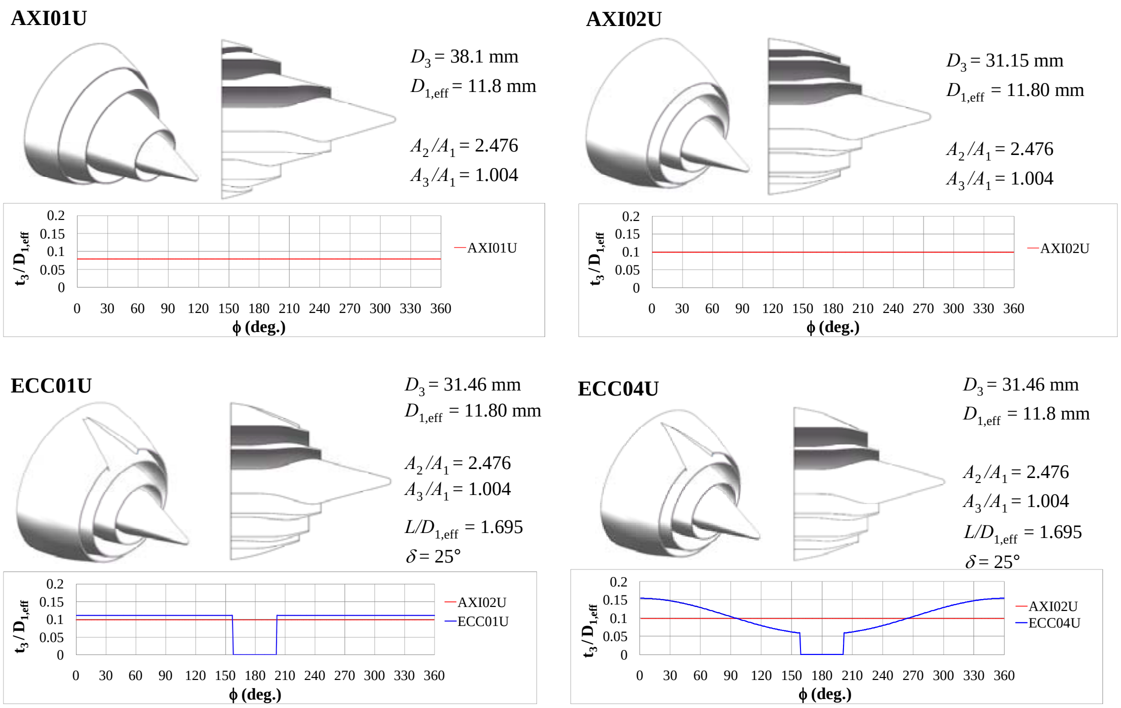

Fig.5 Nozzles associated with cycle points 58230 and 88530.

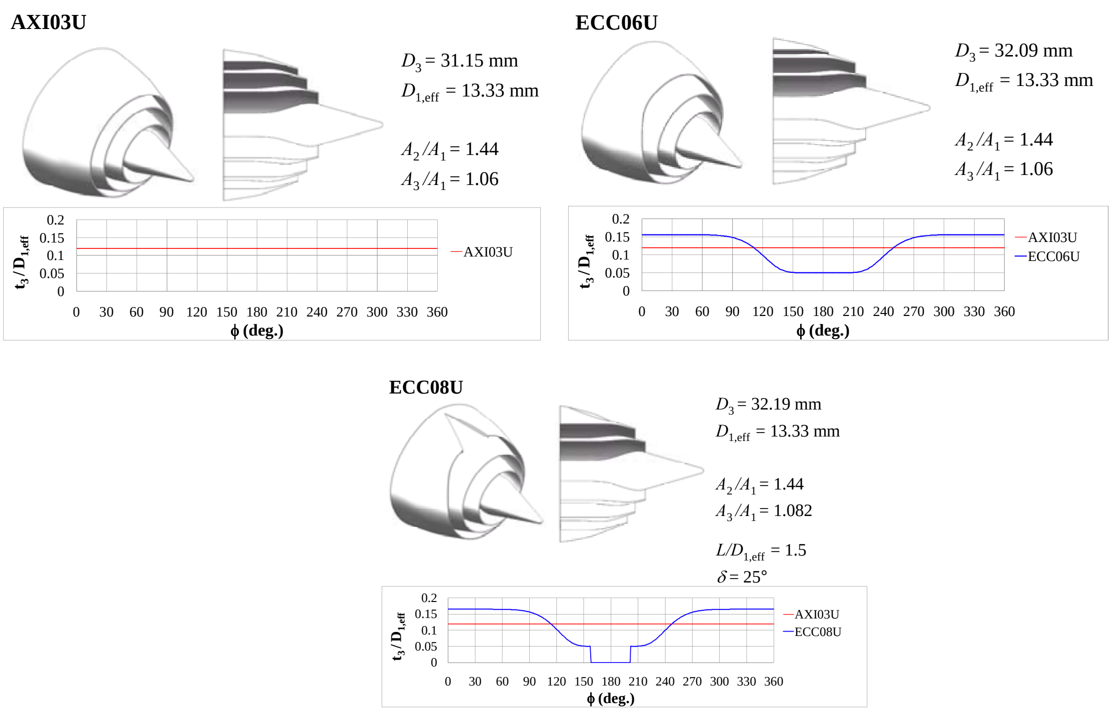

Fig.6 Nozzles associated with cycle point AA530.

C. Aeroacoustic Testing

Noise measurements are conducted in the UCI aeroacoustic facility shown in Fig. 4. The microphone array consists of twenty four 1/8-in. condenser microphones (Bruel & Kjaer, Model 4138) with frequency response up to 120 kHz. Twelve microphones are mounted on a downward arm (azimuth angle $\phi = 0^o$) and twelve were installed on a sideline arm ($\phi = 60^o$). Figure 7 depicts the configuration of the downward arm; the sideline arm is practically identical. On each arm, the polar angle θ ranges approximately from 20^o to 120^o relative to the downstream jet axis, and the distance to the nozzle exit ranges from 0.92 m to 1.23 m. This arrangement enables simultaneous measurement of the downward and sideline noise at all the polar angles of interest. The microphones are connected, in groups of four, to six conditioning amplifiers (Bruel & Kjaer, Model 2690-A-0S4). The 24 outputs of the amplifiers are sampled simultaneously, at 250 kHz per channel, by three 8-channel multi-function data acquisition boards (National Instruments PCI-6143) installed in a Dell Precision T7400 computer with a Xeon quad-core processor. National Instruments LabView software is used to acquire the signals. The temperature and humidity inside the anechoic chamber are recorded to enable computation of the atmospheric absorption. The microphone signals were conditioned with a high-pass filter set at 300 Hz. Narrowband spectra were computed using a 4096-point Fast Fourier Transform, yielding a frequency resolution of 61 Hz. The spectra are corrected for microphone actuator response, microphone free field response and atmospheric absorption, thus resulting in lossless spectra. For the typical testing conditions of this experiment, and for the farthest microphone location, the absorption correction was 4.5 dB at 120 kHz.

This paper covers only the "downward" acoustics, which for asymmetric nozzles is the direction of the thickened tertiary flow. Due to the failure of one downward-oriented microphone in the course of this investigation, there will be some variability in the polar angles covered in the results section.

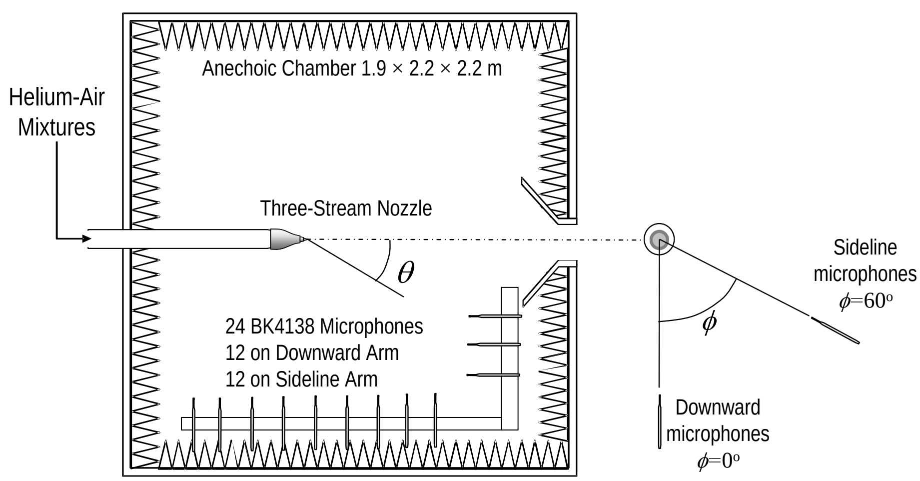

Fig. 7 Aeroacoustic test setup.

III. Computational Approach

The computational fluid dynamics code used here is known as PARCAE[27] and solves the unsteady three-dimensional Navier-Stokes equations on structured multiblock grids using a cell-centered finite-volume method. Information exchange for flow computation on multiblock grids using multiple CPUs is implemented through the MPI (Message Passing Interface) protocol. In its time-averaged implementation, the code solves the RANS equations using the Jameson-Schmidt-Turkel dissipation scheme[28] and the Shear Stress Transport (SST) turbulence model of Menter[29]. The SST model combines the advantages of the k-ω and k-ε turbulence models for both wall-bounded and free-stream flows. The governing equations were solved explicitly in a coupled manner using five-stage Runge-Kutta scheme toward steady state with local time stepping, residual smoothing, and multigrid techniques for convergence acceleration. Only the steady-state solution was considered because we are interested in the time-averaged features of the flow.

The computation encompassed both the internal nozzle flow as well as the external plume. Figure 8 shows the grid for the long-cowl nozzle AXI01U in the vicinity of the nozzle exit. The computational domain extended to 38 jet diameters downstream and 8 diameters radially. As all the configurations were symmetric about the meridian plane, only one-half of the domain was modeled to save computational cost. The typical grid contained 8 million points. The grid was divided into multiblocks to implement parallelization on multiprocesor computers to reduce the convergence time. For the primary, secondary, and tertiary duct flows, uniform total pressure was specified at the inlet surface corresponding to the perfectly expanded exit Mach number. For the ambient region surrounding the nozzle flow, a characteristic boundary condition was defined, and the downstream static pressure was set equal to the ambient pressure. Adiabatic no-slip boundary condition was specified on all nozzle walls.

The code has been used in past research on dual-stream jets, and its predictions have been validated against mean velocity measurements[30]. In addition to providing information on the plume flow field, the code also predicts the aerodynamic performance of the nozzles.

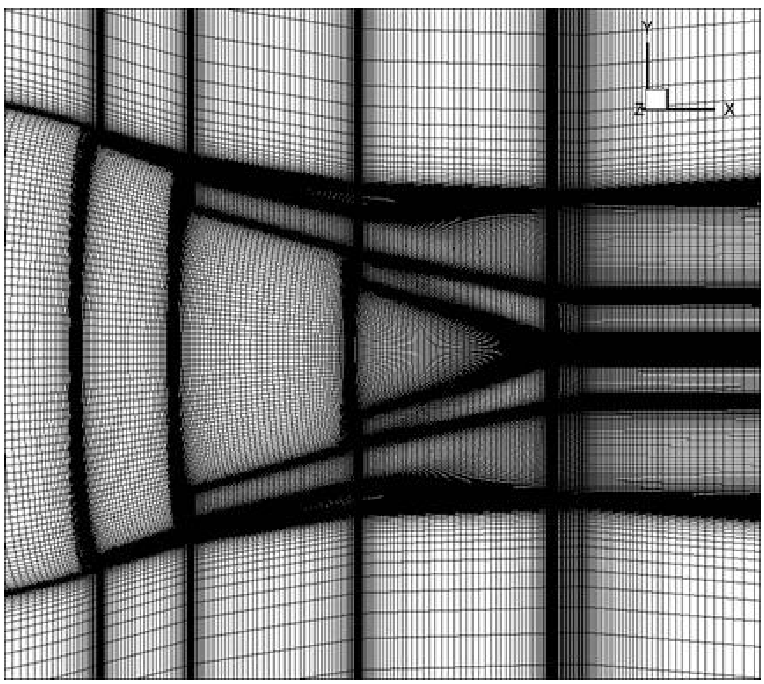

Fig. 8 Example of computational grid near the nozzle exit.

IV. Results

Acoustic results will be presented in terms of the far-field sound pressure level spectra at various polar angles. They will be accompanied by RANS predictions of the turbulent kinetic energy distribution on the symmetry plane.

A. Effect of Tertiary Stream on Coaxial Jet Noise

The presentation of the results begins with an assessment on the effect of the third stream on the acoustics of coaxial jets. Short- and long-cowl nozzles are compared. Figure 9 presents the effect of the tertiary stream on long-cowl nozzle AXI01U operating at cycles 58030 (two-stream) and 58230 (three-stream). Addition of the third stream causes a small decline of the high end of the spectrum at low polar angles.

This indicates that third stream induces changes only very near the nozzle exit plane. For the same cycles, nozzle AXI02U presents nearly identical trends, as shown in Fig. 10. At the higher-thrust conditions 88030/88530, the effect of the tertiary stream on the broadband spectrum is practically negligible for nozzle AXI01U (Fig. 11); however, some tonal noise is evident at cycle 88530. On the other hand, nozzle AXI02U shows some minor reduction across all angles, as shown in Fig. 12.

Figure 13 provides a direct comparison between the long- and short-cowl nozzles at cycle point 88530. The broadband spectra practically collapse, however the long-cowl nozzle (AXI01U) emits some tonal noise as previously noted. It is interesting to note that large-scale NASA experiments at the same condition also showed tonal noise[24]. The reason for the tonal noise is not presently understood, and it is not known if the source of the tones is the same in the UCI and NASA tests.

We gain additional insight into the effect of the third stream by examining contours of the normalized turbulent kinetic energy (k/U_1^2) on the symmetry plane. Potential cores are identified as regions of near-zero TKE bounded by shear layers with finite levels of TKE. Figure 14 shows the TKE distributions at cycle points 58030 and 58230 for long-cowl nozzle AXI01U. Addition of the tertiary stream causes a small reduction in TKE very close to the exit of the secondary duct. Examination of the region close to nozzle exit reveals a very thin and short tertiary potential core. Figure 15 presents the analogous information for short-cowl nozzle AXI02U. Here we observe a modestly enhanced effect of the tertiary stream, with TKE reduction near the nozzle exit and a more pronounced tertiary core. These effects are too minor to induce a noticeable change in the acoustics. However, they suggest that the short-cowl nozzle is a better point of departure for forming asymmetric configurations that are effective in reducing noise.

Two- and three-stream comparisons for the higher-thrust condition AA530 show very similar trends to Fig. 12 and are thus not presented here.

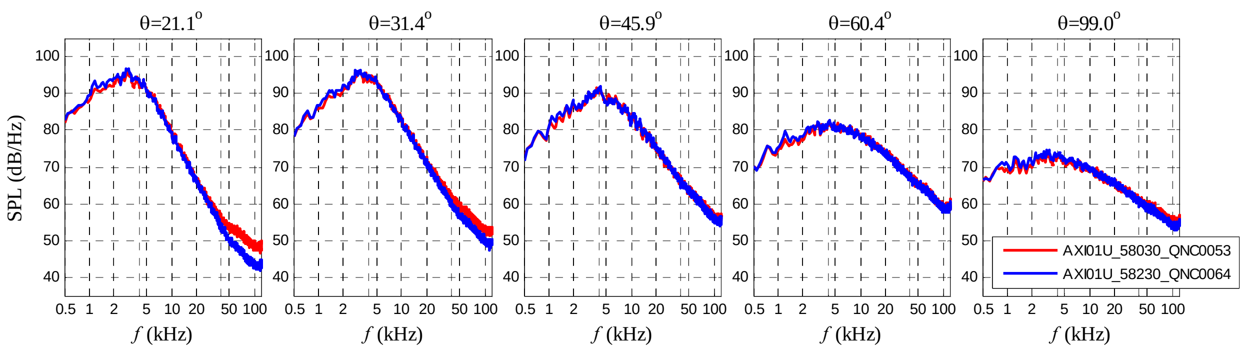

Fig. 9 Effect of the tertiary stream on the acoustics of long-cowl nozzle AXI01U. Cycle points: 58030 (two-stream) and 58230 (three-stream).

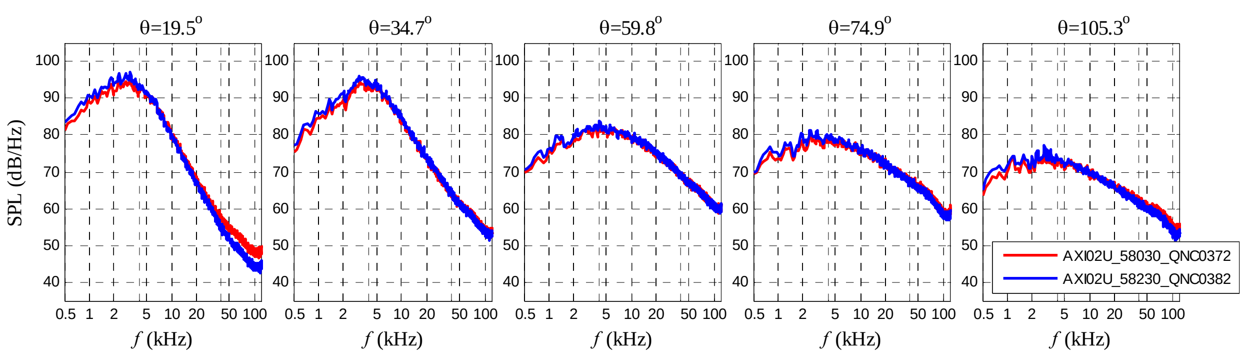

Fig. 10 Effect of the tertiary stream on the acoustics of short-cowl nozzle AXI02U. Cycle points: 58030 (two-stream) and 58230 (three-stream).

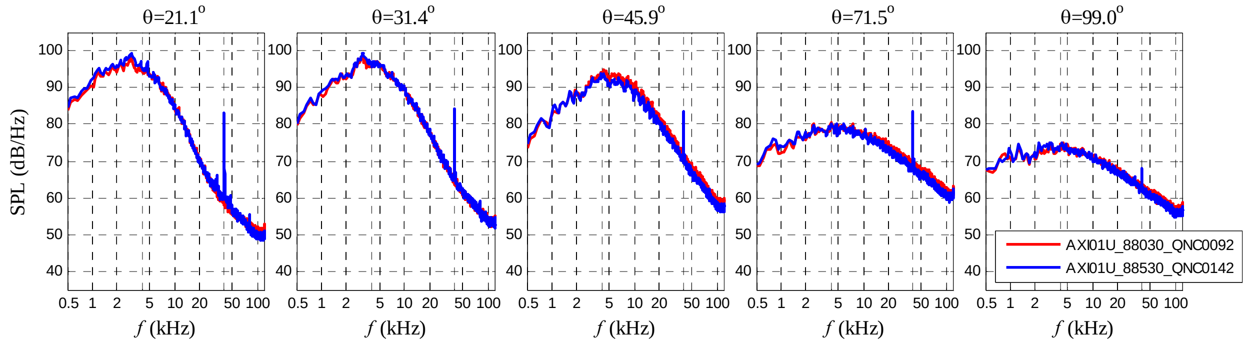

Fig. 11 Effect of the tertiary stream on the acoustics of short-cowl nozzle AXI01U. Cycle points: 88030 (two-stream) and 88530 (three-stream).

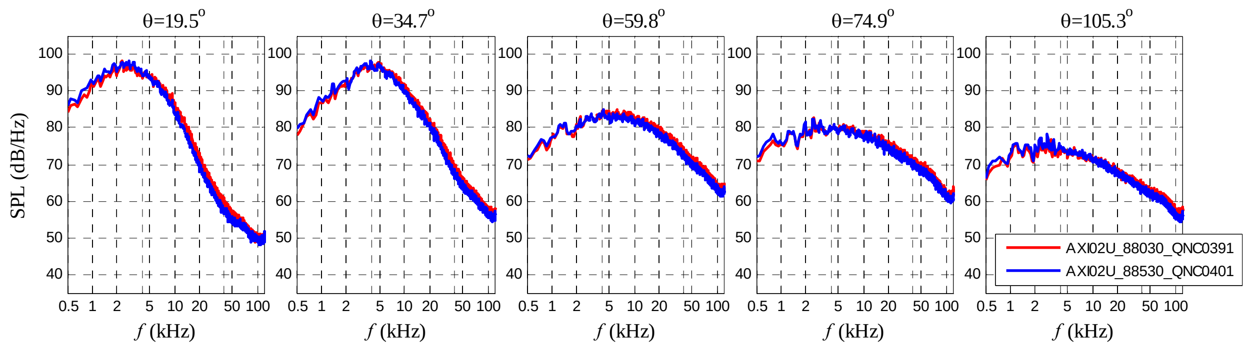

Fig. 12 Effect of the tertiary stream on the acoustics of short-cowl nozzle AXI02U. Cycle points: 88030 (two-stream) and 88530 (three-stream).

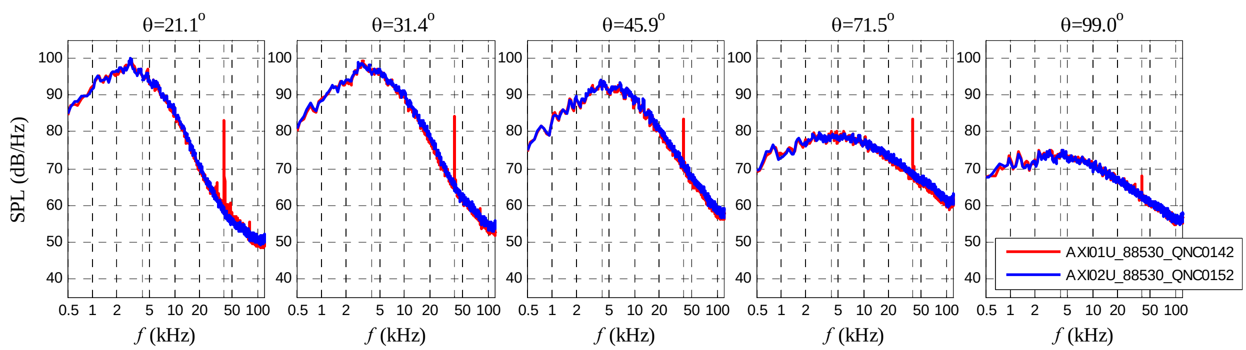

Fig. 13 Comparison between long-and short-cowl nozzles at set point 88530.

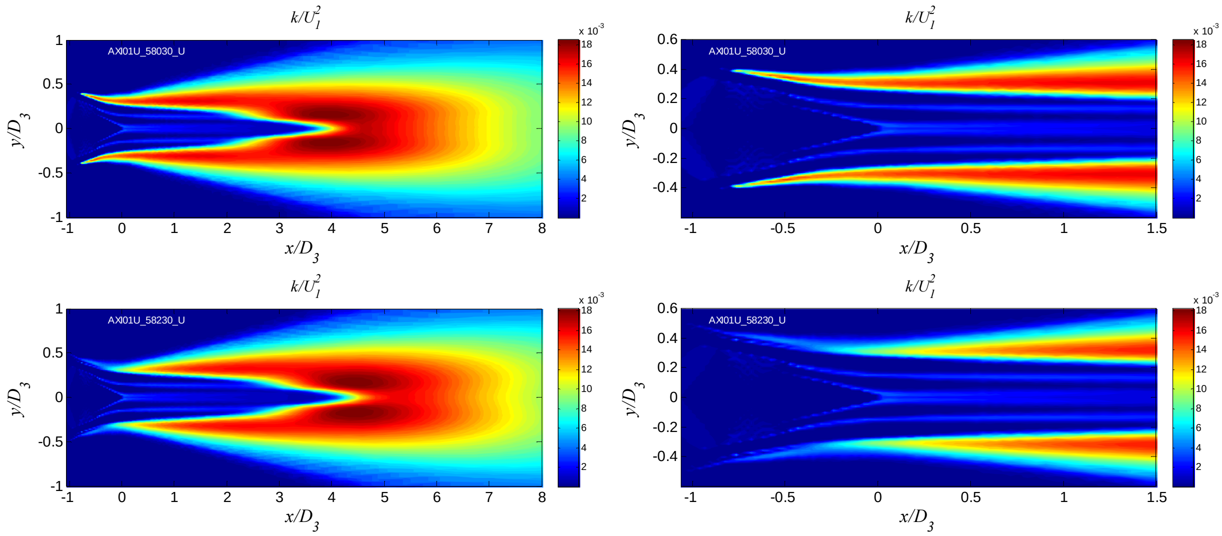

Fig. 14 TKE distributions on the symmetry plane for nozzle AXI01U at cycle points 58030 (two-stream, top) and 58320 (three-stream, bottom). Right column shows details near the nozzle exit.

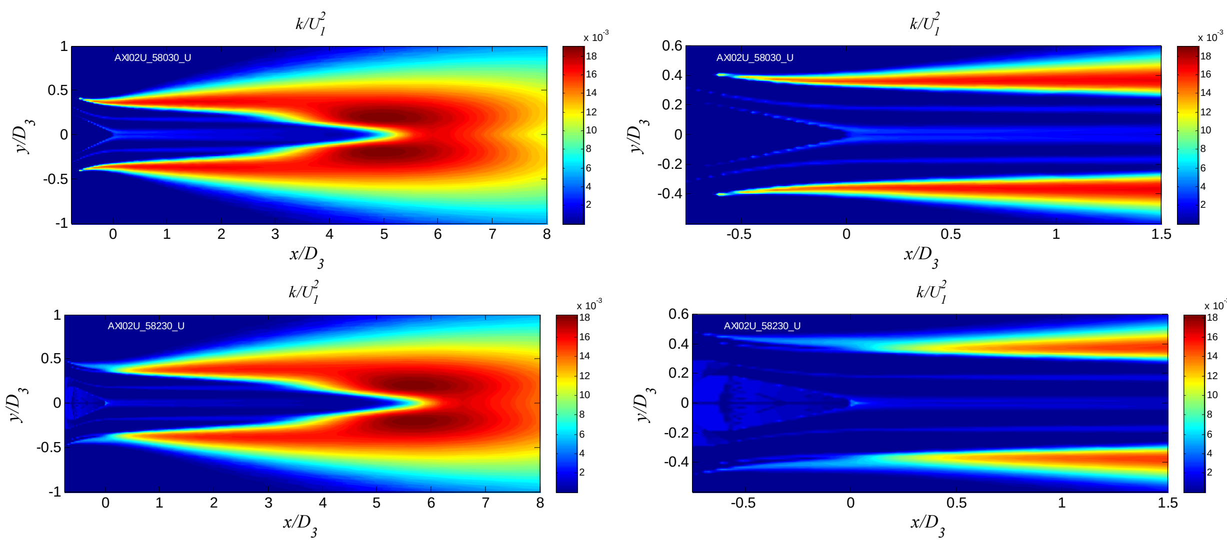

Fig. 15 TKE distributions on the symmetry plane for nozzle AXI02U at cycle points 58030 (two-stream, top) and 58320 (three-stream, bottom). Right column shows details near the nozzle exit.

B. Asymmetric Configurations

As discussed in section II.C, the point of departure for the design of asymmetric arrangements is the short-cowl nozzle. We start with a comparison of nozzles AXI02U and ECC01U at cycle point 58230, shown in Fig. 16. Nozzle ECC01U features a moderate deflection, which offers a distinct but small acoustic benefit in the aft arc. Increasing the thrust to cycle point 88530, Fig. 17, enhances somewhat this benefit, especially at low polar angles. The spectra of nozzle ECC04U, plotted in Fig.18, indicate significant noise reductions in the aft arc, approaching ~5 dB in the medium to high frequency range. This benefit is magnified at the higher thrust cycle point 88540, as shown in Fig. 19. Small amounts of excess noise are measured at the very large polar angles.

The RANS predictions of TKE for nozzles AXI02U, ECC01U, and ECC04U at cycle point 58230 are presented in Fig. 20. Nozzle ECC01U causes a moderate reduction of TKE on the underside of the jet, on the order of 20%. This causes a moderate noise reduction, as seen in Fig. 16. On the other hand, the TKE reduction of nozzle ECC04U is substantial, on the order of 70% in the downward region up to x/D_3=4. The prolonged tertiary core on the lower side of the jet is evident. As a result, noise reduction for ECC04U is significant as shown in Fig. 18.

Considering now the lower bypass ratio cycle point AA530, Fig. 21 plots the spectra for nozzles AXI03U and ECC06U. Reductions on the order of 10 dB are seen for the low polar angles in the medium to high frequency range. Addition of the wedge deflector in nozzle ECC08U increases these reductions to ~ 15 dB, as shown in Fig. 22. Nozzle ECC08U represents one of the most promising configurations investigated in this program.

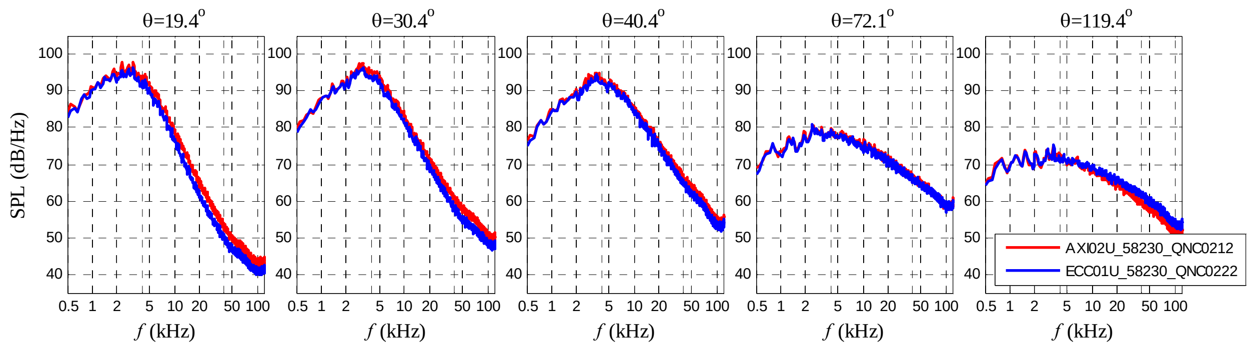

Fig. 16 Comparison between nozzles AXI02U and ECC01U at set point 58230.

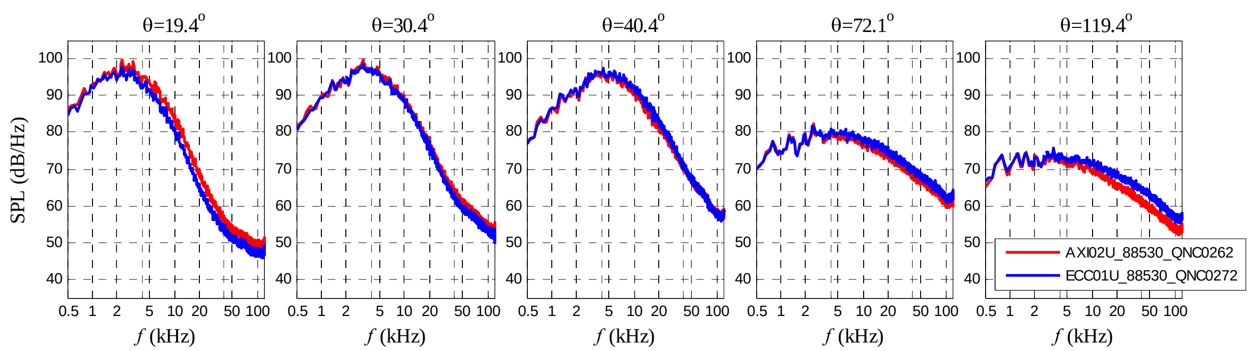

Fig. 17 Comparison between nozzles AXI02U and ECC01U at set point 88530.

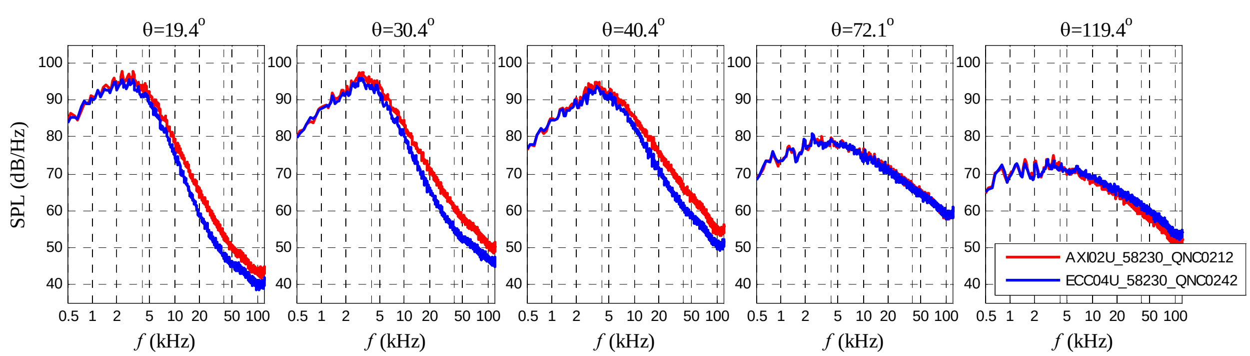

Fig. 18 Comparison between nozzles AXI02U and ECC04U at set point 58230.

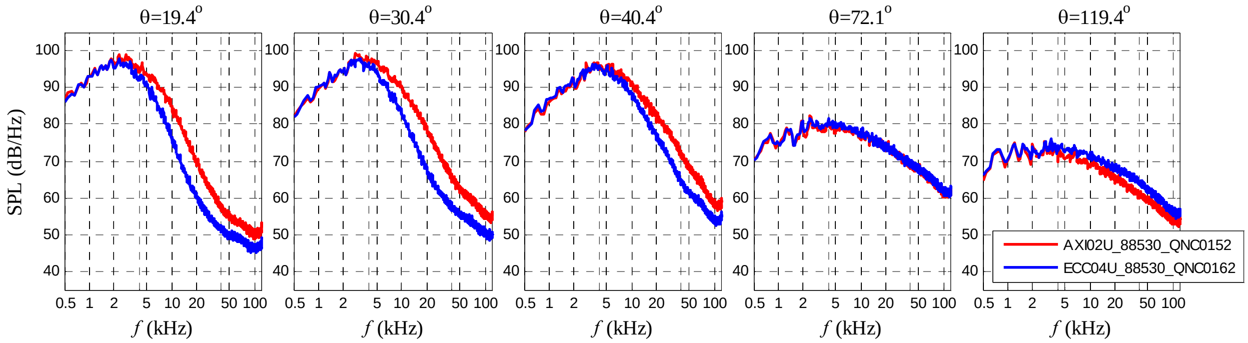

Fig. 19 Comparison between nozzles AXI02U and ECC04U at set point 88530.

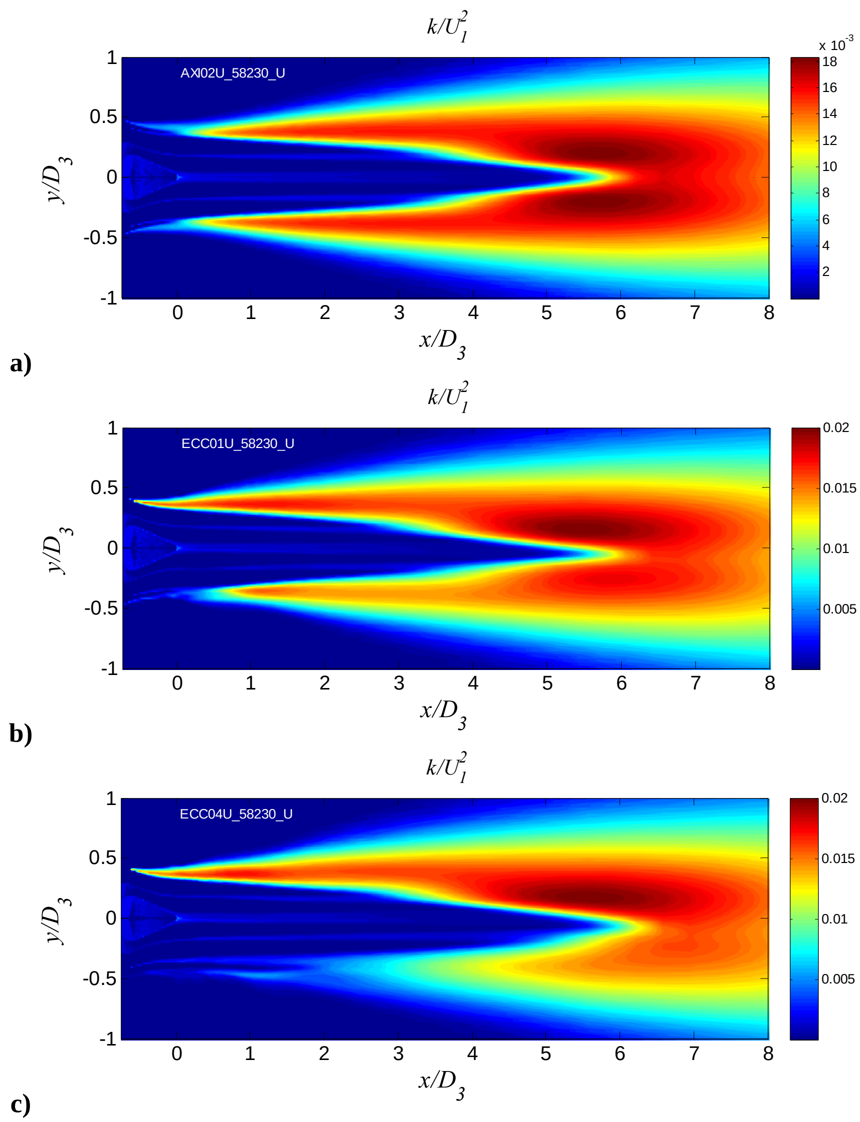

Fig. 20 TKE distributions on the symmetry plane for nozzles: a) AXI01U; b) ECC01U; and c) ECC04U. Cycle point is 58230.

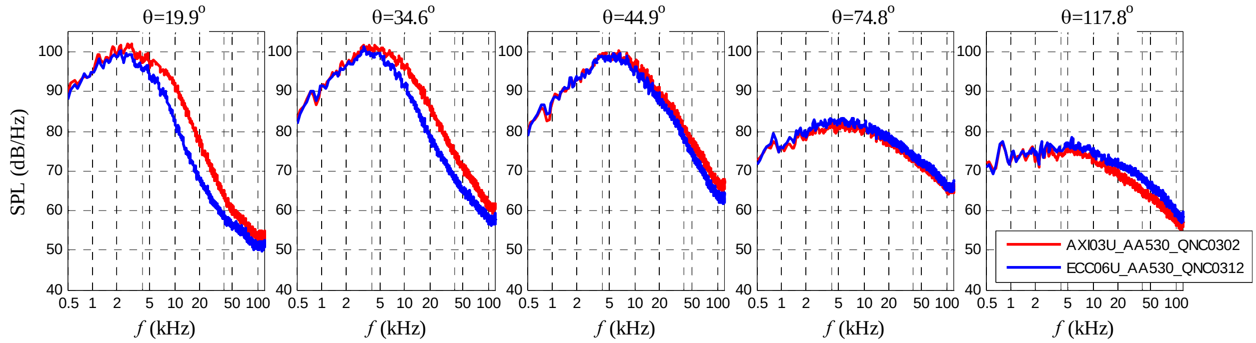

Fig. 21 Comparison between nozzles AXI03U and ECC06U at set point AA530.

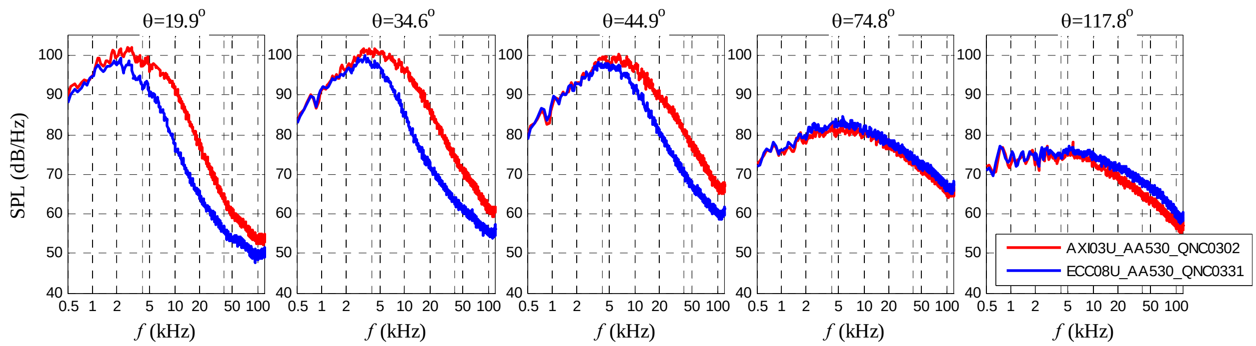

Fig. 22 Comparison between nozzles AXI03U and ECC08U at set point AA530.

RANS results for the TKE of nozzles AXI03U, ECC06U and ECC08U are plotted in Fig. 23. For ECC06U we note the very substantial suppression of TKE on the underside of the jet, which reaches up to about 7 jet diameters. For ECC08U, the underside of the jet appears completely devoid of large values of TKE. The acoustic and RANS results presented in these cases illustrate that large flow-field changes are needed for inducing significant acoustic benefits. It is notable, however, that these changes do not need to be accompanied by significant performance loss. Based on the RANS predictions, the specific thrust loss of nozzle ECC06U, at static conditions, is only 0.011%.

C. Evidence of Mach Wave Radiation

Strong Mach wave radiation has been connected to the skewness of the far pressure field[31,13,32]. In the course of the acoustic experiments it was noted that the microphone time traces appeared skewed, particularly near the angle of peak emission. Here we make a brief comment on the distribution of pressure skewness for the higher-thrust condition AA530.

The polar directivity of the normalized skewness is plotted for nozzles AXI03U and ECC08U in Fig. 24. For the baseline coaxial jet (AXI03U), the skewness peaks near the angle of peak emission, $\theta \approx 45^{o}$. The peak value of 0.5 is large enough to indicate some non-linear steepening of the waveforms, which is associated with strong Mach wave radiation. It is not large enough to suggest significant "crackle" noise typically emitted by hot, supersonic, single-stream jets[31]. The asymmetric tertiary stream in nozzle ECC08U reduces the skewness significantly for all angles less than ~45 deg. Now the peak value is near 0.35 at $\theta \approx 60^{o}$. The reduction in skewness is consistent with suppression of Mach wave emission or, more generally, reduction in radiation efficiency. The reduction in skewness is not as dramatic as that seen in high-speed jets with eccentric coflow[13], which suggest the potential for even stronger noise reduction with proper shaping of the tertiary, and possibly the secondary, streams.

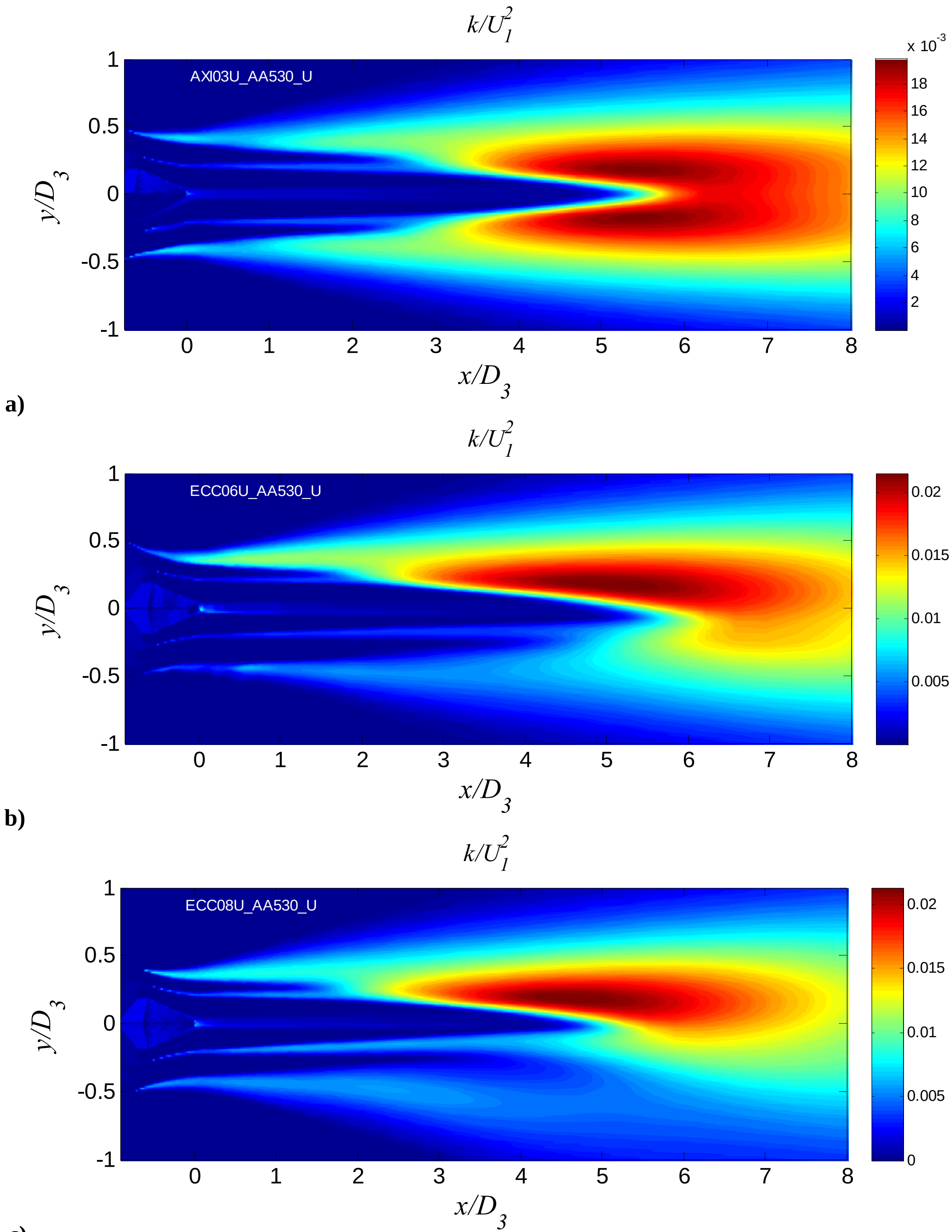

Fig. 23 TKE distributions on the symmetry plane for nozzles: a) AXI03U; b) ECC06U; and c) ECC08U. Cycle point is AA530.

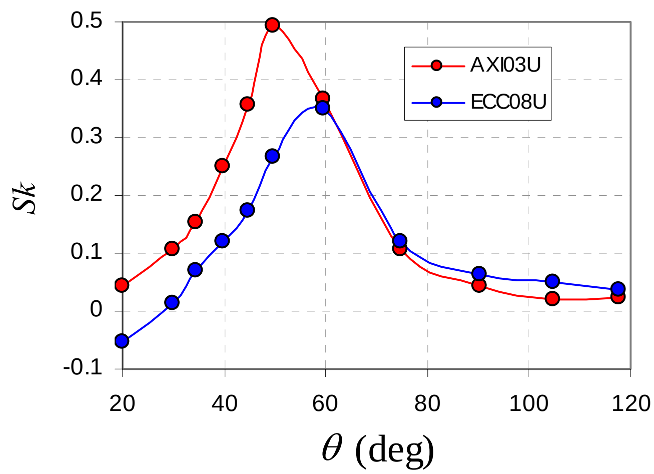

Fig. 24 Polar directivity of the skewness of the far pressure field for nozzles AXI03 and ECC08U.

V. Conclusions

We presented the initial phase of an investigation of three-stream nozzle concepts with potential to reduce takeoff noise of future commercial supersonic aircraft. The concepts were evaluated at realistic cycle conditions in a subscale acoustic facility. Combined bypass ratios (secondary plus tertiary) ranged from 3.6 to 6.0. Computations solving the Reynolds-Averaged Navier-Stokes equations provided insight into the changes in the flow field that can impact noise generation.

The investigation encompassed long- and short-cowl nozzles, as well as asymmetric arrangements where the third stream was concentrated in the downward azimuthal direction. In coaxial configurations, addition of the third stream makes a very small impact on the noise emission, with a small benefit at high frequencies in the aft arc. This benefit is more evident in short-cowl nozzles, where for the same area the thickness of the tertiary annulus is slightly larger and the tertiary exit is in closer proximity to the primary exit. The basic fluid mechanics of the problem are such that, for coaxial configurations, the tertiary stream has very limited extent to induce any significant modification to the flow field, and consequently to the acoustic field. This is due to the thinness of the tertiary layer, combined with a low nozzle pressure ratio for the tertiary stream. The area ratio for the tertiary flow would need to be very large for it to induce large changes, but this is unfeasible for the engine cycles envisioned.

Asymmetric delivery of the tertiary stream shows strong potential for noise reduction, but the detailed flow lines of this delivery are crucial. Means to induce asymmetry study encompassed partially offset nozzles and wedge-shaped deflectors, used individually and in combination. Wedge-shaped deflectors with moderate deflection angle, used in isolation, induce moderate noise reduction. Offsetting partially the nozzle leads to more significant noise reductions. Combined, these two concepts lead to strong noise reduction in the direction of the thickened flow. The reduction increases with increasing specific thrust of the nozzle. For the lower bypass-ratio cycle point, reductions reached ~15 dB in the medium to high-frequency sound emitted in the aft arc. Skewness distributions of the far-field pressure suggest the presence of significant Mach wave radiation in the baseline coaxial jet and its suppression when the tertiary flow is asymmetric.

Acknowledgment

We acknowledge the support by NASA Cooperative Agreement NNX14AR98A, monitored Dr. James Bridges.

References

1. Morgenstern, J., Norstrud, N., Sokhey, J., Martens, S., and Alonso, J.J., "Advanced Concept Studies for Supersonic Commercial Transports Entering Service in the 2018 to 2020 Period - Phase I Final Report," NASA/CR--2013-217820.

2. Simmons, R.J., "Design and Control of a Variable Geometry Turbofan with an Independently Modulated Third Stream," Ph.D. Dissertation, The Ohio State University, 2009.

3. Morris, P.J. and McLaughlin, D.K., 2013, "High Speed Jet Noise Reduction - Past Progress and Future Possibilities", AIAA Paper 2013-0006, Jan. 2013.

4. Dosanjh, D., Ahuja, J., Bassiouni, M., Bhutiani, P., "Supersonic Jet Noise Suppression by Coaxial Cold/Heated Jet Flows," AIAA Paper 76-507, July 1976.

5. Tanna, H. K., "Coannular Jets-Are They Really Quiet and Why?" *Journal of Sound and Vibration*, Vol. 72, No. 1, 1980, pp. 97-118.

6. Tanna, H.K., and Morris, P.J., "The Noise from Normal-Velocity-Profile Coannular Jets," *Journal of Sound and Vibration*, Vol. 98, No.2, 1985, pp. 213-234.

7. Fisher, M.J., Preston, G.A., and Bryce, W.D. "A Modelling of the Noise from Simple Coaxial Jets, Part 1: With Unheated Primary Flow," *Journal of Sound and Vibration*, Vol. 209, No. 3, 1998, pp. 385-403.

8. Dahl, M.D. and Papamoschou, D., "Supersonic Coaxial Jets: Noise Predictions and Measurements," *AIAA Journal*, Vol. 38, No.4, 2000, pp. 584-591.

9. Zaman, K.B.M.Q., and Dahl, M.D., "Noise and Spreading of a Subsonic Coannular Jet - Comparison with Single Equivalent Jet," *AIAA Journal*, Vol. 45, No.11, 2007, pp. 2661-2670.

10. Bogey, C., Barre, S., Juve, D., and Bailly, C., "Simulation of a Hot Coaxial Jet: Direct Noise Prediction and Flow-Acoustics Correlations," *Physics of Fluids,* Vol. 21, No. 3, 2009, Article 035105.

11. Papamoschou, D., "Mach Wave Elimination in Supersonic Jets," *AIAA Journal*, Vol. 35, No.10, 1997, pp. 1604-1611, pp. 154-160.

12. Papamoschou, D. and Debiasi, M., "Noise Measurements in Supersonic Jets Treated with the Mach Wave Elimination Method," *AIAA Journal*, Vol. 37, No.2, 1999, pp. 380-387.

13. Papamoschou, D. and Debiasi, M., "Directional Suppression of Noise from a High-Speed Jet," *AIAA Journal*, Vol. 39, No.3, 2001, pp. 380-387.

14. Papamoschou, D., "Engine Cycle and Exhaust Configurations for Quiet Supersonic Propulsion," *Journal of Propulsion and Power*, Vol. 20, No. 2, 2004, pp. 255-262.

15. Zaman, K.B.M.Q., "Noise- and Flow-Field of Jets from an Eccentric Coannular Nozzle," AIAA Paper 2004-0005, Jan. 2004.

16. Papamoschou, D., "New Method for Jet Noise Suppression in Turbofan Engines," *AIAA Journal*, Vol. 42, No.11, 2004, pp. 2245-2253.

17. Brown, C.A., Bridges, J.E., and Henderson, B., "Offset Stream Technology Test - Summary of Results," AIAA Paper 2007-3664, May 2007.

18. Dippold, V., Foster, L., Wiese, M. "Computational Analyses of Offset-Stream Nozzles for Noise Reduction," *Journal of Propulsion and Power*, Vol. 25, No. 1, Jan.-Feb. 2009.

19. DeBonis, J.R., "RANS Analyses of Turbofan Nozzles with Internal Wedge Deflectors for Noise Reduction," *Journal of Fluids Engineering*, Vol. 131, April 2009, Article 041104.

20. Papamoschou, D. and Rostamimonjezi, S., "Modeling of Noise Reduction for Turbulent Jets with Induced Asymmetry," AIAA Paper 2012-2158, June 2012.

21. Papamoschou, D., Xiong, J., and Liu, F., "Reduction of Radiation Efficiency in High-Speed Jets," AIAA Paper 2014-2619, June 2014.

22. Papamoschou, D., Johnson, A.D., and Phong, V., “Aeroacoustics of Three-Stream High-Speed Jets from Coaxial and Asymmetric Nozzles,” *Journal of Propulsion and Power*, Vol. 30, No. 4, 2014, pp. 1055-1069.

23. Henderson, B., “Aeroacoustics of Three-Stream Jets,” AIAA Paper 2012-2159, June 2012.

24. Henderson, B., Leib, S.J., and Wernet, M., “Measurements and Predictions of the Noise from Three-Stream Jets,” AIAA Paper 2015-3120, June 2015.

25. Papamoschou, D., “Acoustic Simulation of Coaxial Hot Air Jets Using Cold Helium-Air Mixture Jets,” *Journal of Propulsion and Power*, Vol. 23, No.2**,** 2007, pp. 375-381.

26. Papamoschou, D., “Noise Suppression in Moderate-Speed Multistream Jets”, AIAA Paper 2002-2557, June 2002.

27. Xiong, J., Johnson, A., Liu, F., and Papamoschou, D., “Body Force Model for the Aerodynamics of Inclined Perforated Surfaces,” *AIAA Journal*, Vol. 50, No.11, Nov. 2012. pp. 2525-2535.

28. Jameson, A., Schmidt, W., and Turkel, E., “Numerical Solutions of the Euler Equations by Finite Volume Methods Using Runge-Kutta Time Stepping Schemes,” AIAA Paper 1981-1259, Jan. 1981.

29. Menter, F., “Two-Equation Eddy-Viscosity Turbulence Models for Engineering Applications,” *AIAA Journal*, Vol. 32, No. 8, 1994, pp. 1598–1605.

30. Xiong, J., Nielsen, P., Liu, F., and Papamoschou, D., “Computation of High-Speed Coaxial Jets with Fan Flow Deflection,” *AIAA Journal*, Vol. 48, No.10, 2010, pp. 2249-2262.

31. Ffowcs Williams, J. E., Simson, J., and Virchis, V. J., “Crackle: an Annoying Component of Jet Noise,” *Journal of Fluid Mechanics*, Vol. 71, Pt. 2, 1975, pp. 251–271.

32. Gee, K.L., Neilsen, T.B., Atchley, A.A., “Skewness and Shock Formation in Laboratory-Scale Supersonic Jet Data,” *Journal of the Acoustical Society of America*, Vol. 133, May 2013, EL491-497.